Journal of Advanced Research 39 (2022) 61–71

Contents lists available at ScienceDirect

Journal of Advanced Research

journal homepage: www.elsevier.com/locate/jare

"Plasmonic Nanomaterials": An emerging avenue in biomedical and biomedical engineering opportunities

Yasaman-Sadat Borghei [a,*], Saman Hosseinkhani [b,*], Mohammad Reza Ganjali [c]

[a] Department of Nanobiotechnology, Faculty of Biological Sciences, Tarbiat Modares University, Tehran, Iran
[b] Department of Biochemistry, Faculty of Biological Sciences, Tarbiat Modares University, Tehran, Iran
[c] Center of Excellence in Electrochemistry, Faculty of Chemistry, University of Tehran, Tehran, Iran

HIGHLIGHTS

- This review links between physicochemical aspects and their biomedical applications.
- It lists the possible medical applications of plasmonic nanoparticles.
- It presents future directions of plasmonic nanoparticles in clinical translations.
- It talks about the different pathways that have been studied and where they are lacking.

GRAPHICAL ABSTRACT

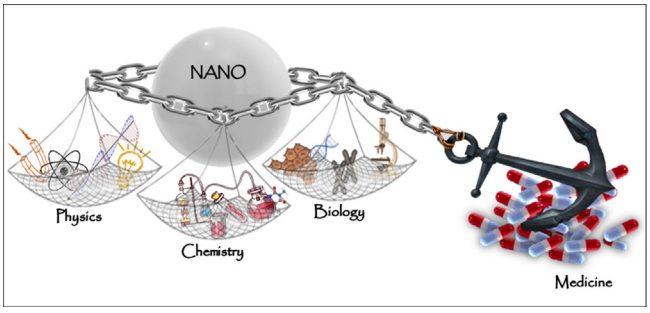

ARTICLE INFO

Article history:
Received 9 September 2021
Revised 7 November 2021
Accepted 11 November 2021
Available online 20 November 2021

Keywords:
Nanomaterial
Physicochemical properties
Tissue engineering
Biomedical

ABSTRACT

Background: Plasmonic nanomaterials as noble metal-based materials have unique optical characteristic upon exposure to incident light with an appropriate wavelength. Today, generated plasmon by nanoparticles has received increasing attention in nanomedicine; from diagnosis, tissue and tumor imaging to therapeutic and biomedical engineering.

Aim of review: Due to rapid growing of knowledge in the inorganic nanomaterial field, this paper aims to be a comprehensive and authoritative, critical, and broad interest to the scientific community. Here, we introduce basic physicochemical properties of plasmonic nanoparticles and their applications in biomedical and tissue engineering The first part of each division explain the basic physico-chemical properties of each nanomaterial with a graphical abstract. In the second part, concepts by describing classic examples taken from the biomedical and biomedical engineering literature are illustrated. The selected case studies are intended to give an overview of the different systems and mechanisms utilized in nanomedicine.

Key Scientific Concepts of review: In this communication, we have tried to introduce the needed concepts of plasmonic nanomaterials and their implication in a particular part of biomedical over the last 20 years. Moreover, in each part with insist on limitations, a perspective is presented which can guide a researcher how they can develop or modify new scaffolds for biomedical engineering.

Introduction

Plasmon is an optical phenomena generated by light when the incident light with an appropriate wavelength strikes the noble metal surface (at the dielectric interface), the conducted electrons

Peer review under responsibility of Cairo University.
* Corresponding authors.
E-mail addresses: y.borghei@modares.ac.ir (Y.-S. Borghei), saman_h@modares.ac.ir (S. Hosseinkhani).

https://doi.org/10.1016/j.jare.2021.11.006
2090-1232/

gain energy and start oscillating. This collective movement of free electrons on the metal surface (plasmon) is limited to the particle sizes around 300 nm [1–3].

What is surface plasmon resonance (SPR)? These oscillating free electrons make an electromagnetic field on the noble metal surface. As the energy of the both electromagnetic field (induced electromagnetic field and incident electromagnetic field) be the same, the resonance condition is accomplished, which is called SPR or propagation SPR. Based on noble metal size, there are two types of SPR: Propagation SPR (PSPR) and Localized SPR (LSPR) [4–6]. *PSPR* is usually generated on metal thin films and surface plasmon resonance can propagate along the metal/dielectric surface up to hundreds of micrometers. Since this resonance can be affected by biomolecules, this property has been used in sensing [7]. In SPR, plasmons propagate in the x-, y- and z-directions along the thick metal/dielectric interface. SPR is very sensitive to the variations in surface layer leads to shifts in the plasmon resonance condition (SPR angle) which make it a powerful detection technology. In a commercial SPR, incident light is employed by using a high-reflective index glass prism in the Kretschmann geometry of the attenuated total reflection (ATR) method (although other methods such as waveguide coupling, diffraction grating, or optical fibers can also be used). The reflective index changes in the metal film layers (*i.e.*, gold, silver) in response to analyte (which depends on proportion to the molecular mass of the analyte attached to the surface). In SPR imaging, the reflected light is captured by a charge-coupled device (CCD) camera for more imaging analysis. The measurement conducted by SPRI is performed at a constant wavelength and a constant angle. The amount of brightness in each of the flow cells indicates the amount of analyte attached.

LSPR is generated when the noble metals are smaller than the incident wavelength (it means that they are nanosized noble metal particles), in which surface plasmon resonant frequency strongly depends on the composition, size, geometry, dielectric environment and separation distance of nanoparticles (NPs) [8–11]. LSPR is used for localized induced electromagnetic waves that are trapped on the metal surface (typically on the order of 30 nm). The LSPR properties such as extinction peak (extinction = absorption + rayleigh scattering) of metal nanostructures can be tuned over a wide wavelength range by varying different parameters, including the type, size, shape, dimension, geometry, ….

So, the extinction peak depends on different parameters that can be used as a basis for the development of colorimetric sensors with high sensitivity [12–14]. Specially gold, silver and copper NPs exhibit LSPR effects in the visible wavelength. So they can be used as colorimetric reporter to analyte detection [15].

As discussed above, after irradiating light to NPs, the resonant oscillation of transmission electrons at the metal/dielectric interface have finite lifetimes. Following which the LSPR relaxes (the excited plasmon decay) either radiative or nonradiative (Fig. 1) [16–18].

Radiative decay

The radiative decay (by emitting a photon) processes either through inducing electromagnetic field near the surface of the nanostructures (near-field effect) or by light scattering (far-field effect). During radiative decay procedures the plasmonic NPs act as a secondary light source. This section will describe the two mechanisms of electromagnetic field enhancement and light (rayleigh) scattering that categorized within radiative effects, shown in Fig. 1 [16–19].

Local electromagnetic-field enhancement (in the near field)

It was explained that after irradiation of light into plasmonic NPs results in electromagnetic fields near the NP surface which may enhance during LSPR decay. Intense local EM fields, strengthen some optical phenomena such as Raman scattering, infrared absorption and the local refractive index. Accordingly, several methods have been developed that are explained further [16,17,20].

Surface-enhanced Raman spectroscopy and imaging (SERS & SERSI). After light (monochromatic) strikes the molecule, some photons can get scattered elastically (with the same energy of irradiated light) and inelastically (With different energy than irradiated light). Inelastically scattering related to the specific vibrational energy levels of each molecule, known as Raman Effect (discovered by Sir C. V. Raman) [21]. One of the most important applications of plasmonic NPs is to enhance the Raman signal (SERS). Hence the plasmonic NP is called SERS substrate. To use SERS as a spectroscopy and imaging tool, the rayleigh scatters should be filtered after the sample was irradiated with laser (coherent source) and data processing by a charge-coupled device (CCD) camera (Fig. 2A) [21–23]. SERS can be used as an analytical tool in two platforms (Fig. 5A): intrinsic/direct mode and extrinsic/indirect mode. As shown in Fig. 2B, C, D, you can see examples of SERS in diseases diagnosis [24,25].

The local refractive index. Reflective LSPR based system employs the sensitivity of the plasmon frequency to changes in local refractive index at the nanoparticle surface (Fig. 3A). Binding of an analyte to the surface of the NP leads to variation in refractive index at the nanoparticle surface that in turn shifts the LSPR peak frequency [4,10,27].

Surface-enhanced infrared absorption (SEIRA). The near field effect of LSPR relaxation due to plasmon excitation can be employed for surface-enhanced vibrational energy level (Raman signal or infrared absorption spectroscopies) (Fig. 3B). So surface enhanced infrared absorption (SEIRA) spectroscopy can provide data about located analyte in close to plasmonic NPs, because each molecule has unique vibrational absorptions in the IR fingerprint region [28,29].

Light scattering (in the far field)

As shown in Fig. 1, LSPR decays either radiatively by rayleigh scattering into the far field (occurs mainly for large plasmonic NPs (often >50 nm)) [17,30]. Accordingly, plasmonic NPs can be used in Dark Field Microscopy (DFM) and as a contrast agent in medical imaging.

Dark Field Microscopy. In LSPR relaxes most photons get scattered elastically (Rayleigh scattering), hence DFM was developed in plasmonic NPs sensing. A typical configuration for a DFM is described in Fig. 3C [31].

Contrast agent. These plasmonic NPs bear great promise in x-ray based biomedical imaging (radiology) (Fig. 4) such as radiography, mammography and computed tomography (CT). The x-ray imaging is based on the difference in density between two tissues. Contrast agents are materials with a high atomic number (z) that play a main role in imaging with high contrast by introducing high density media into the body. Therefore, high-Z nanoparticles as contrast agents may permit x-ray based imaging at lower doses and with high sensitivity and specificity [33–36]. Nanoparticle-based X-ray contrast agents must be designed to meet the requirements like "Go where we want", "Do not harm along the way", "Stay where we want" and "Show what we want". As shown in Fig. 4C, in radiography, functionalized AuNPs enter the bloodstream and can only reach the tumor tissue, after intravenous injection [37].

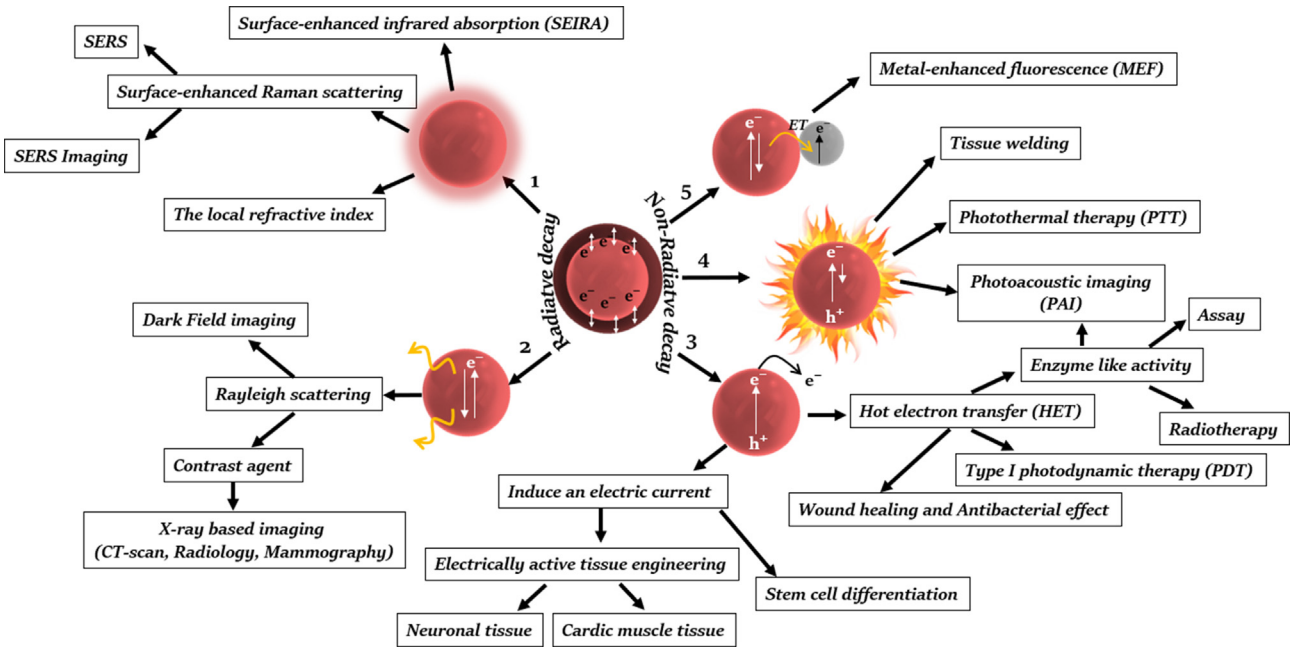

Fig. 1. Different mechanisms for LSPR relaxation: Radiative decay by (1) Local electromagnetic-field enhancement (in the near field), or by (2) Light scattering (in the far field). Non-Radiative decay by (3) Hole-hot electron pair, or by (4) Plasmonic heating, or by (5) Plasmon Resonance Energy Transfer (PRET). (In some reports, (1) local electromagnetic-field enhancement and (5) PRET are classified in one category.)

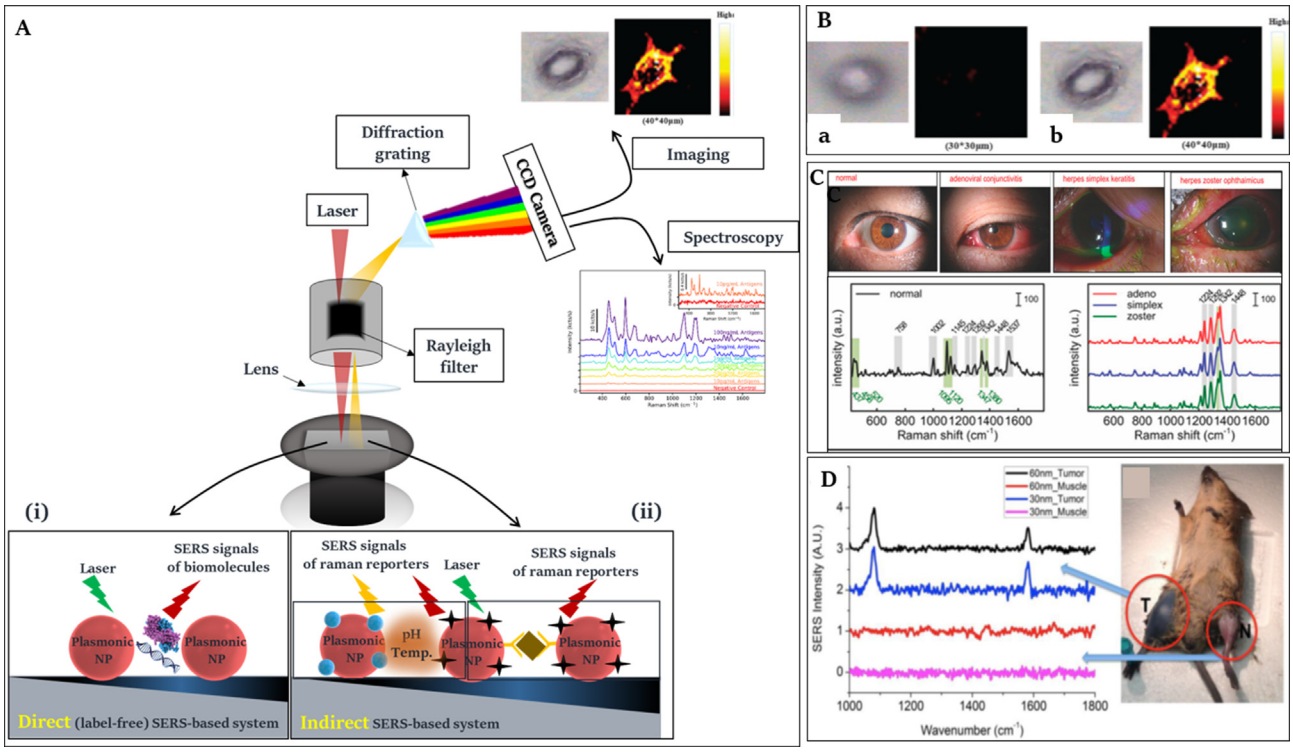

Fig. 2. (A) SERS-based biosensors can be used as a spectrum or imaging in two modes: (i) label-free direct detection mode which is based on the adsorption of the molecule to the SERS substrate and the SERS signal fingerprints of molecule and (ii) Raman label-enabled indirect detection mode is based on the use of recognition element (such as antibody, aptamer, . . .) on the SERS substrate to bring target molecule close to the NPs surface and the strong Raman signals of the Raman reporter molecules (Raman tags). (B) Indirect SERS-based microscopic imaging technique for targeting and imaging specific cancer markers distributed on the cell membrane by using MP (as Raman tag)/antibody/gold nanorod. (a) Cell (no markers), (b) cell (yes marker). The left pictures are bright-field images, while the right images are Raman mapping images at the 1095 cm^{-1} peak of Raman reporter MP [22]. (C) Direct, label-free cell membrane biomarker detection in bodily fluid using SERS. Raman spectrum of (left) a normal eye fluid, and (right) fluid from the three types of eye infections [21]. (D) *In vivo* indirect SERS-based spectra of 30-nm and 60-nm gold nanostar nanoprobes with pMBA reporter. Specific SERS peaks can be detected at 1067 and 1588 cm^{-1} in the tumor, but not in the normal muscle. Mouse with primary sarcomas 3 days after 30-nm GNS injection. Significant nanostar accumulation can be seen in the tumor (T), but not in the normal leg muscle of the contralateral leg (N) [26].

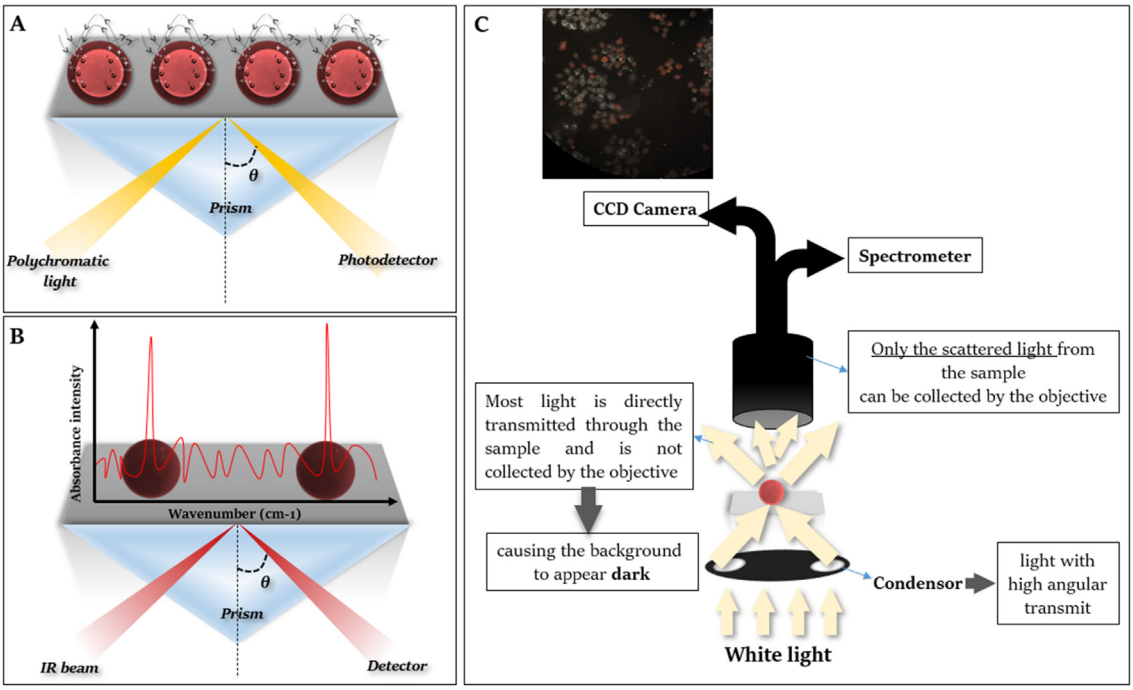

Fig. 3. (A) In a commercially available tool, the local refractive index-based LSPR signal, incident light is used by using a high-reflective index glass prism. The reflective index (refractive angle) changes in response to analyte. (B) In SEIRA spectroscopy, first plasmonic NPs are located at the crystal surface by different methods including sputtering, lithography and vapor phase or wet chemical deposition. Then, analyte sample are ran at the surface and the interaction between analyte and plasmonic NPs makes a difference in the intensity of IR absorption. (C) In the DFM, the condenser permits white light (Halogen lamp) to pass from sample with high angular. So the transmission light is not collected by the objective, causing the background to appear dark. Only rayleigh scattered light from the sample can be collected by objective to produce the image by CCD or by a spectrometer. (inset) MCF-7 cells after treatment with gold nanostructures [32].

Or as shown in Fig. 4D, the AgNPs can be identified as a good contrast agent in mammography [38].

Computed Tomography (CT) works like conventional x-ray radiography, except that the x-ray tube and detector rotate around the examined body part. As can be seen in Fig. 4E, Gold nanoparticles (GNPs) are able to increase contrast compared to control (mouse without GNPs). In addition, mouse with targeted GNPs can act as an effective strategy to improve the amount and residence time of contrast agents in tumors compared to mouse with non-targeted GNPs [39]. In Vivo CT contrast properties of gold/silver alloy NPs were studied using a mouse without tumors (Fig. 4F). Contrast was observed in different organs with a long circulation half-life [40].

Non-radiative decay

As briefly illustrated in Fig. 1, LSPR relaxation is a non-radiative decay processes. This section will describe the three mechanisms of hole-hot electron pair, plasmonic heating, plasmon resonance energy transfer (PRET) and their medical applications which fall under non-radiative effects [30,41].

Hole-hot electron pair

During a non-radiative plasmon decay, energetic relaxation generates high-energy quantum hot charge electrons (carriers) in the conduction band and a hole in the valence band form a hydrogen-like state due to the mutual Coulomb interaction. Such a state is called hole-hot electron pair and about plasmonic NPs, it is driven by intra- and inter-band excitation of the conduction electrons. Here, 'hot electron' with high energy (more than fermi level) either causes an electric current (induce an electric current) or it can be injected (hot electron transfer (HET)) and initiate external chemical reaction [30,42].

Hot electron transfer (HET)

In the hot-electron injection mechanism, these charge carriers (the hot electrons and holes) are sufficient in energy (from the Fermi level to the work function) and lifetime transfer to a nearby chemical species to initiate a single or multistep external chemical processes such as enzyme like activity and radiosensitizer (for Radiotherapy) [30].

Enzyme like activity. In plasmonic NPs, hot electrons with high kinetic energy (i.e., 1–3 eV) can be generated by the decay of surface plasmons at a femtosecond timescale after exposure to light. The plasmonic NPs as the source of electrons by LSPR exhibit the intrinsic catalytic activity that the extent of this activity depends on the flow of hot electrons generated at plasmonic NPs surface. The plasmonic NPs have been developed rapidly because of their catalytic activities and high chemical stability. Since their activity is similar to natural enzymes like peroxidase, oxidase or catalase, they are also called nanozymes [41,43–46]. The plasmonic NPs (by generated hot electrons) can break down hydrogen peroxide (H_2O_2) (in peroxidase mimetic activity: the O—O bond of H_2O_2 might be broken up into double $HO^{\cdot}$ radical) or molecular oxygen (O_2) (in oxidase mimetic activity: the O—O bond might be broken up into double $O^{\cdot}$ radical) and produce radicals that can convert reduced substrate to oxidized form and H_2O [44–46]. Now, if this substrate is a chromogenic substrate, then by converting to the oxidized form, a color change is created that can be used in bioanalytical methods in a broad range from lateral flow assay [47,48], ELISA and cell immunoassay to the detection of analytes. In all three cases, nanozymes were used instead of enzyme to conjugate with recognition element (antibody, aptamer,...). They can also have catalase like activity, through which hydrogen peroxide is consumed and oxygen bubbles are produced [47].

The antimicrobial effect of nanozyme was investigated on gram-positive and negative bacterial strains. As it is known, nano-

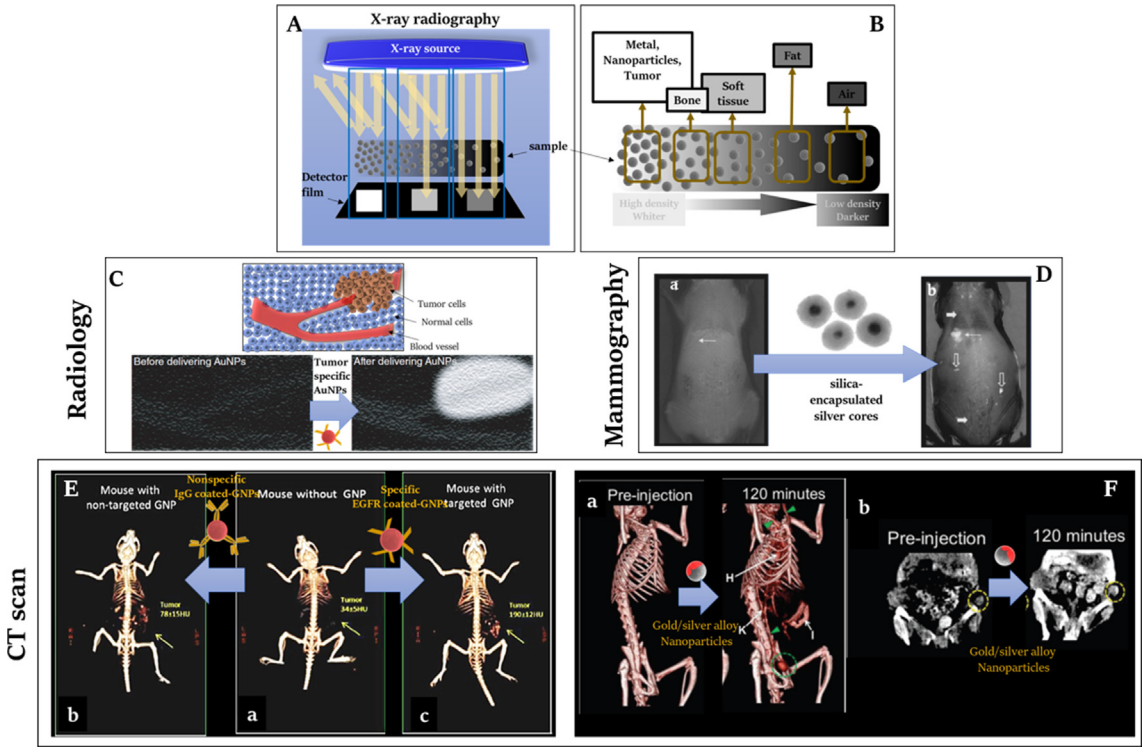

Fig. 4. (A) The x-ray beams leave the x-ray tube, pass through the matter and hit a phosphorus film/detector. The whiteness (=density) depends on the amount of X-ray radiation passing through the matter. (B) The more X-rays are absorbed and scattered by high atomic number matter (or high densities) and the x-ray beams do not reach the detector. (C) Schematic display the functionalized AuNPs as x-ray contrast agents able to target and transport to the specific tumor *in vivo*. So it must increase the x-ray attenuation of the tumor tissue compared with surrounding tissues. (D) The mammography images of mice immediately after subcutaneous injection of the saline (as control) (a) and the silica@Ag contrast agent (b). the site of injection is indicated with a long arrow. (E) *In vivo* CT images of a mouse the Squamous-cell carcinoma before GNP injection (a), a mouse 6 h post-injection of nonspecific Immunoglobulin G (IgG)-GNP as a passive targeting experiment (b) and a mouse 6 h post-injection of anti-epidermal growth factor receptor (EGFR)-coated GNPs as an active targeting experiment (c). (F) *In vivo* CT imaging with GSAN: (a) 3D volume rendered CT images of a mouse (without a tumor) injected with alloy NPs, (b) 2D CT images of a tumor-bearing mouse showing accumulation of alloy NPs in the tumors (yellow circles). (For interpretation of the references to color in this figure legend, the reader is referred to the web version of this article.)

zyme and hydrogen peroxide alone have no antimicrobial effect, but their synergistic effect have shown antimicrobial effect through the peroxidase activity of nanozyme and the production of reactive oxygen species [49,50].

Radiotherapy. Radiation therapy (radiotherapy or RT) remains an important piece of cancer treatment along with surgery and chemotherapy. Radiotherapy uses an ionizing radiation, such as X-ray, which converts water molecules into reactive oxygen species (ROS) in a radiolysis reaction, thus high level of radicals cause an extended damage to tumor cells [51,52]. Because ionizing radiation can damage other organs, so a low dose of radiation should be used, which means less radiation is absorbed in the tumor microenvironment. On the other hand, due to the hypoxic conditions in the tumors, less ROS is produced by radiolysis. Therefore, to solve these problems, it is better to use radiosensitizers such as plasmonic NPs, which in addition of a high atomic number (high-z) can increase the rate of radiation absorption in the tumor, can also increase the amount of produced O_2 due to catalase activity (Fig. 5A) [51].

Wound healing and Antibacterial effect. The wound healing and antimicrobial effects of some plasmonic NPs are caused by the higher chemical reactivity of generated hot electrons and due to higher surface area to volume ratio, leading to the increased formation of ROS [53–56]. Radical superoxide is formed by one-electron reduction of molecular oxygen. Plasmonic NPs can act as electron donors to molecular O_2 leading to the radical reactive superoxide, next the superoxide starts a cascade of radical forming reactions. The antibacterial effect (Fig. 5B) of plasmonic NPs is also related to the production of ROS because they can damage DNA, proteins and gram positive and negative cell walls by using radical reactions [55].

Wound healing involves several stages of coagulation (forming a blood clot), inflammation (release of chemicals by injured cells resulting in leaking fluid into tissue by blood vessels, which makes the tissue swelling), proliferation, and matrix and tissue remodeling. To achieve speed recovery in wound healing with minimal scarring, it needs to decrease cytokines like interleukin-6 (IL-6) and TGF-β mRNA and increase in other cytokines like interferon-γ (IFN-γ) production [57,58]. Some plasmonic NPs, especially silver nanoparticles (AgNPs) use in wound healing by decreasing inflammation through cytokine modulation and achieve better cosmetics. For example as shown in Fig. 5C, in the burn wound site treated with AgNPs, mRNA levels of TGF-β were decreased and about IL-10, VEGF, and IFN-γ were increased and so the wound healing process accelerated. It was also found fewer neutrophils in the treated wound on day 7 (Fig. 5C, b). This suggests a weakened inflammatory response at the wound area after treatment with AgNPs [58].

Type I photodynamic therapy (PDT). Photodynamic therapy (PDT) is a photochemical-based treatment that combines light with a light-sensitive drug (photosensitizer). Upon illumination with visible/near-infrared light, the photosensitizer generates radical reactive superoxide, which can react with intracellular biological substrates, initiating an apoptotic or necrotic processes and finally leading to cell death. In recent years, plasmonic NPs have been used as a photosensitizer in PDT, because they can generate singlet oxygen by the initially created "primary hot electrons" after irradiation with light in their plasmon resonance band [52,59,60]. As can be seen in Fig. 5D, to demonstrate the potential of these nanostruc-

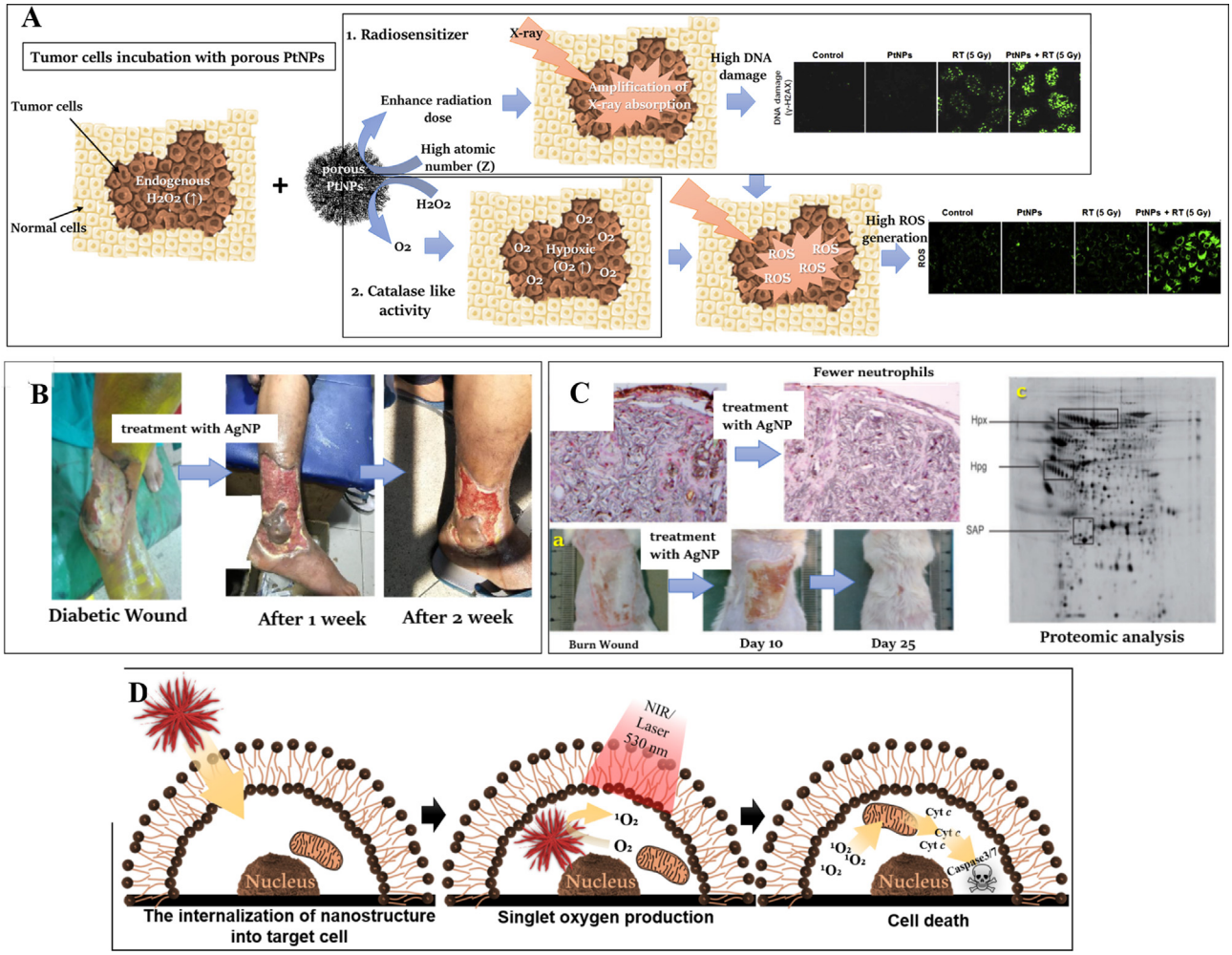

Fig. 5. (A) Tumor cells have high level of endogenous H_2O_2 and low oxygen levels (hypoxia). Due to dual function of porous platinum nanoparticles (radiosensitizer and catalase like activity), after incubation of porous platinum nanoparticles with tumor cells, the nanoparticles on the one hand will be able to increase the amount of radiation absorption (due to their high-z) and as a result, the damage to the DNA increases. On the other hand, it can consume endogenous H_2O_2 and increase the amount of O_2. So the amount of ROS increases, after irradiation. (B) Diabetic Wound after first debridement and application of magnesium sulphate in surrounding skin was treated with AgNPs [55], and (C) AgNPs accelerate burn wound healing in mouse after treatment and achieve superior cosmetic outcome (a), and immunohistochemical staining of wound for neutrophils (pink spots) on day 7 after burn injury before and after treatment with AgNPs (b), and expression of the serum protein markers (hemopexin (Hpx), haptoglobin (Hpg), and serum amyloid protein component P (SAP)) of burn injury by proteomic analysis. The levels of protein markers in serum after treatment with AgNPs returned to nearly normal levels after day 10 (c). (D) For PDT, firstly gold nanostructure would be able to interact with target cells and also capable to produce cytotoxic singlet oxygen under irradiation. These reactive oxygen species (ROS) act as a key factor in programmed cell death (apoptosis). (For interpretation of the references to color in this figure legend, the reader is referred to the web version of this article.)

ture as a light-sensitive drug, its capability of entering the target cell, ROS production upon NIR irradiation and cell fate must be shown [32,61].

Induce an electric current

The injection of hot electrons generated by plasmonic NPs into media is being extensively investigated for many applications such as improving in regeneration of electrogenic tissues like cardiac and neuronal tissues and involving in stem cell differentiation pathway [57,62].

Electrically active tissue (cardiac and neuronal) engineering. A complex process is needed for tissue engineering and regeneration, which should start with the engineered scaffolds. These scaffolds, along with giving physical support, provide cell adhesion, growth and proliferation to functioning units (tissue). However, they have shown limitations that nanostructures have recently been used to overcome, and especially plasmonic NPs are used for engineering electrogenic tissues due to their conduction properties [57,63].

Cardiac tissue engineering. The goal of cardiac tissue engineering is to achieve functional tissue patches in vitro and then implant it to the damaged myocardium to start regeneration [64]. In general, the best design is to use a nonimmunogenic scaffold with efficient electrical coupling between adjacent cells. To address these challenges, it is better to use the patient's own biomaterials as scaffolds to prevent an adverse immune response after transplantation and use of plasmonic nanoparticles to improve transmissions of intercellular electrical signals. An example is shown in Fig. 6A [65].

Neuronal tissue engineering. Development of neurites formation and growth has important challenge in regenerative and engineering of neuronal tissues. It was found that silver nanoparticles to serve as platforms for nerve regeneration and lead to a significantly enhanced neurites outgrowth (Fig. 6B). Silver nanoparticle, in addition to the morphological effect, has the antibacterial effect and so it has become a suitable nanomaterial for neuronal repair with a dual activity, as its antibacterial effects improves regeneration of a damaged region in central nervous system [66,67].

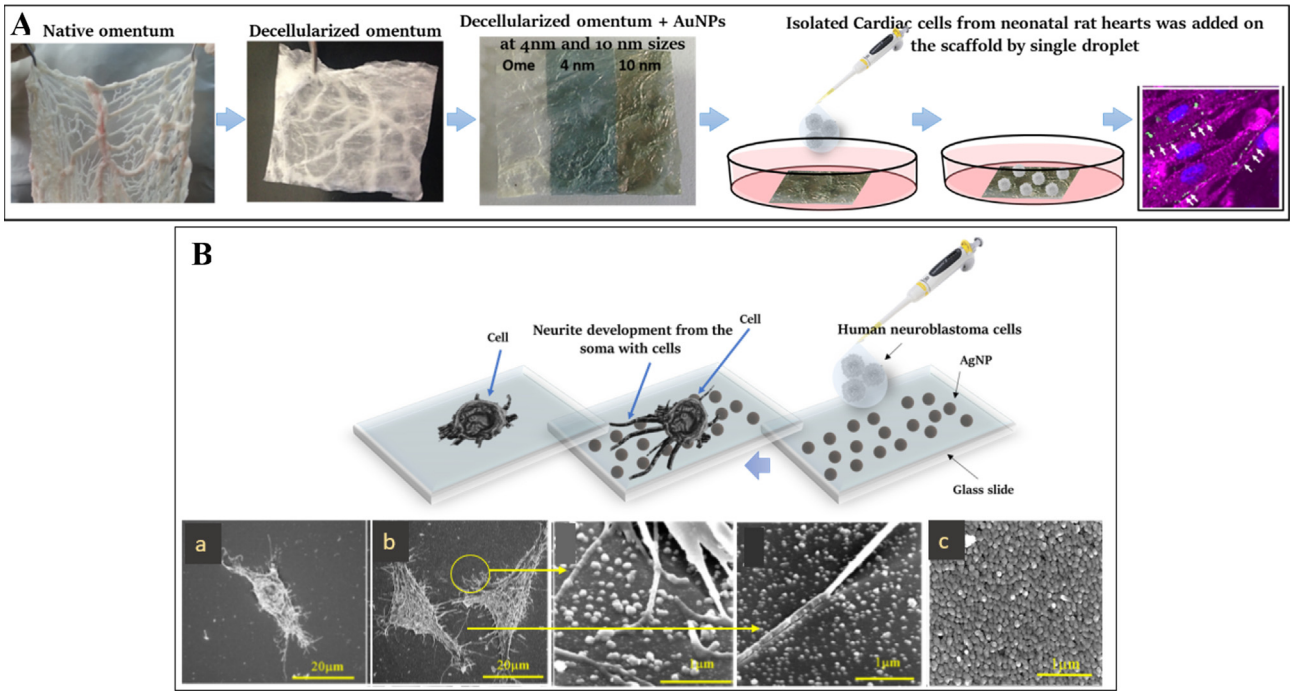

Fig. 6. (A) Schematic engineering of cardiac tissue. First, omental tissue is isolated from the patient and it became acellular. Then AuNPs with different sizes were deposited onto the acellular omentum (as a scaffold). After that, cardiac cells were cultured on the scaffold. On day 5, cardiac patches were immunostained for α sarcomeric actinin (pink color), a protein related to cell contraction, and connexin 43 (green color), related to electrical coupling between adjacent cells. Blue color is nuclei. (B) Growth of neuron cells on the coated substrate with AgNPs and HRSEM images of neuroblastoma cells on uncoated glass (a) and on coated glass with AgNPs at different scale bar (b), HRSEM image of the glass substrate after coating with AgNPs (c). (For interpretation of the references to color in this figure legend, the reader is referred to the web version of this article.)

Stem cell differentiation. Stem cells have important role in tissue engineering and regeneration due to their ability to differentiate into diverse lineages and cell types. Conductive plasmonic nanostructures have been shown to increase the proliferation and differentiation of cells like neurons, osteoblasts, and cardiomyocytes [68,69]. For example, AuNPs have been used with scaffold to promote stem cell differentiation due to their ability to convey electrical signals. Studies show that plasmonic NPs including AgNPs and AuNPs promoted the osteogenic differentiation (Fig. 7A) and inhibited the adipogenic differentiation [70].

For example as shown in Fig. 7B, the potential of AgNPs in osteogenesis was used to form the callus and the subsequent bone fracture healing. For this purpose, AgNPs may cause the migration of MSCs and fibroblasts to the fracture area and with an inductive process, they induce MSCs to proliferate and differentiate to osteoblasts [71].

Also the ability of AuNPs as osteo-conductive agents was used for dental implants. Thus as shown in the Fig. 7C, it was visually observed that the bone density on the surface of Ti–AuNPs was enhanced as compared with bare Ti group 3 weeks after implantation [72].

Plasmonic heating

Plasmonic NPs can convert the absorbed light into heat via a series of nonradiative processes. Under the excitation of incident light, plasmonic NPs give rise to generation of hot electrons with temperatures as high as 1000 K. These excited carriers relax by a series of energy transformation process successively (that are not mentioned here) resulting in a temperature increase of the medium. The easiest and fastest way to identify the plasmonic heating effect is to measure the temperature around plasmonic NPs [42,73].

The plasmonic heating is more effective in small plasmonic NPs (usually < 30 nm) and is used for photothermal therapy, tissue repair and other photo-thermal catalytic reactions [74,75].

Photothermal therapy (PTT). Photothermal therapy involves the use of light and a photoabsorber to generate heat from light absorption for therapeutic purposes. In some cases, PTT is preferable to PDT because oxygen is not required at PTT, which may be of importance when a tumor is in a hypoxic condition. Plasmonic NPs mediated-photothermal therapy involves the irradiation of a NP to generate localized heat. Intracellular heating perform once the NP has been taken up within the cell while extracellular heating occurs by attaching to the external membranes of target cells [9,74,76]. To investigate the *in vivo* PTT performance, it was done in mice bearing primary sarcomas. The tumors treated with gold nanostar and laser irradiation, in addition to reaching a temperature about 50 °C after only 4 min of treatment do not have any measurable size one day after PTT [26].

Photoacoustic imaging (PAI). Photoacoustic imaging (optoacoustic imaging) involves the photoacoustic effect and ultrasound waves (Fig. 8A). In the photoacoustic effect, the absorption of the pulsed light/radiofrequency wave by sonophore leads to local heating and thermoelastic expansion which can generate wideband ultrasonic waves (photoacoustic waves) [77–79]. Many molecules can be utilized as endogenous or exogenous sonophore, as long as they absorb light [35,80]. As shown in Fig. 8B, C, plasmonic NPs as an exogenous sonophore was used for contrast enhancement.

Tissue welding. For wound closure and tissue welding, there are different conventional methods including sutures, staples and biological glues that each one has its own drawbacks, for example in the case of suturing, in addition to the fluid and air leakage, there is a possibility of physical damage to the surrounding tissue or about biological glues such as cyanoacrylates strongly adhere to tissues

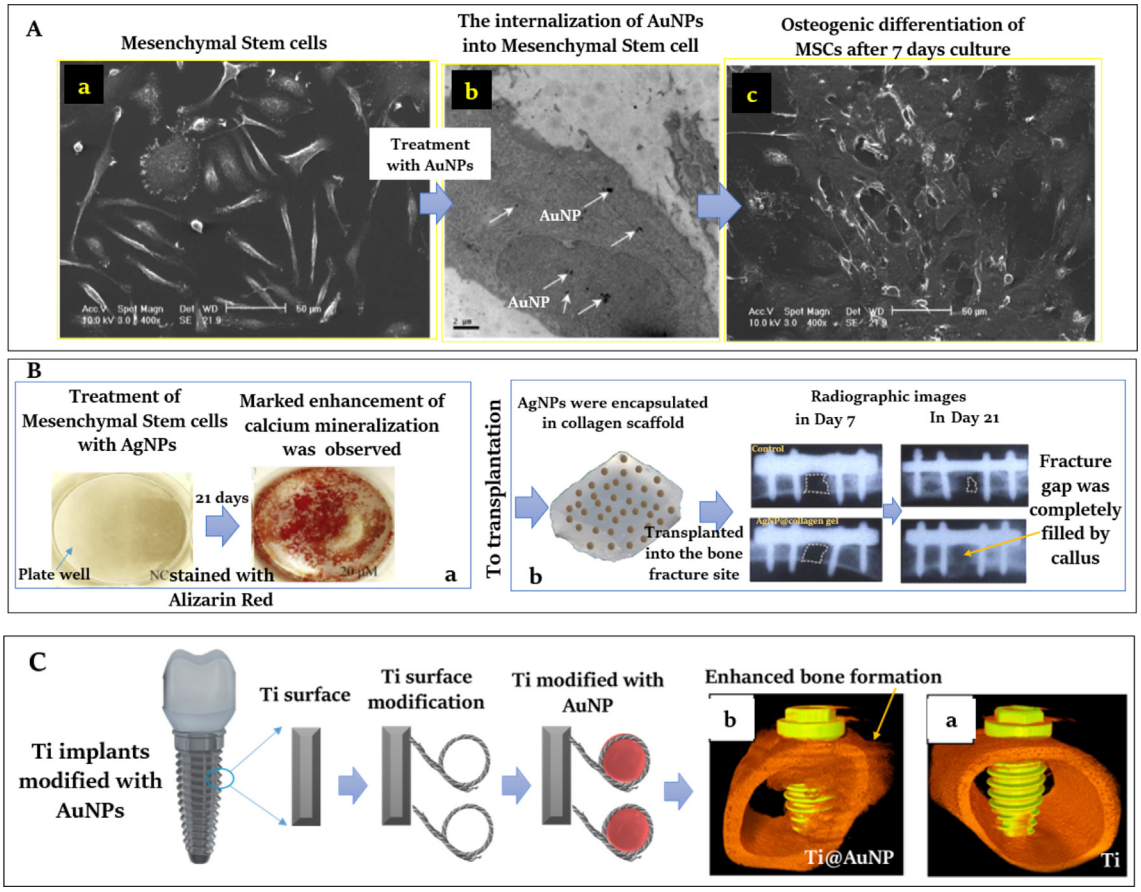

Fig. 7. (A) SEM image of MSCs after 7 days culture (a), TEM images of the internalization of AuNPs into MSCs after treatment MSCs with AuNPs (b), and SEM image of cultured MSCs in the presence of AuNPs, after 7 days. (B) mouse MSCs were cultured in osteogenic differentiation medium with AgNPs for 21 days and then stained with Alizarin Red S (stain calcium deposits) (a), to *in vivo* studies, AgNPs were encapsulated in scaffold and transplanted into the bone fracture site. The healing process was investigated by radiography. (broken line shows the un-filled fracture gap) (C) First, titanium implant surface coated with 3-Mercaptopropyl-AuNPs and then the bare Ti (a) and Ti-AuNPs (b) were implanted into tapped holes of the rabbit femora and both groups were analyzed for bone density by μCT analysis. (For interpretation of the references to color in this figure legend, the reader is referred to the web version of this article.)

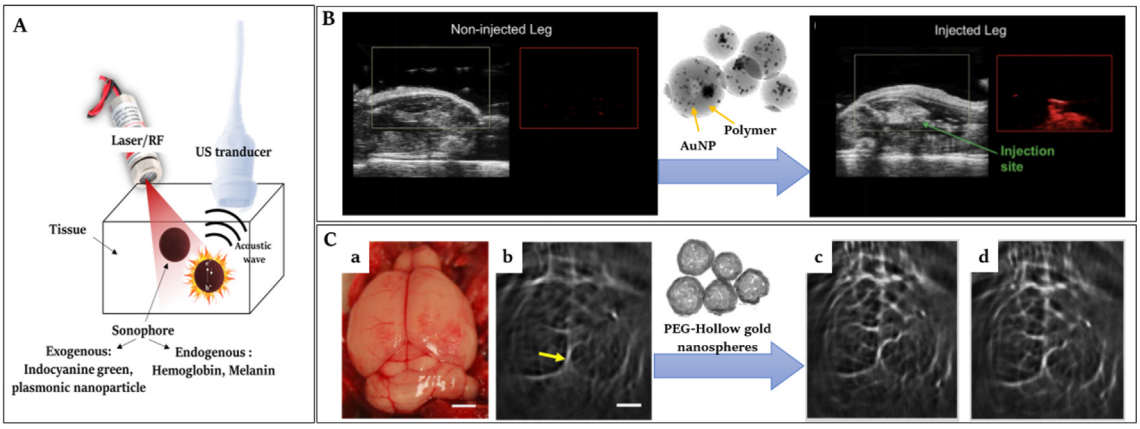

Fig. 8. (A) Principles of PAI. During PAI, pulses of light/RF illuminate the target tissue. Sonophore absorbs light and transient heating gives rise to acoustic waves which are detected by US transducer. (B) PA contrast arising from AuNPs encapsulated into biodegradable polymer injected in the tight muscle of mice. The grayscale images are ultrasound images (left) acquired simultaneously with the PA images (right) [81]. (C) Open-skull photograph of the mouse brain cortex (a), PA imaging of a mouse brain *in vivo* before (b), 5 min (c) and 2 h (d) after the intravenous injection of nanosphere and NIR light irradiation [82].

and have toxic side effects. Recently, laser tissue welding (LTW) or laser tissue soldering (LTS) have been used for tissue repair [76,83]. In fact, the laser generates local thermal at tissue and leads to loss of the structure of the collagenous fibers in the connective tissue, and subsequent cooling leads to reorganization of the fibers. This method provide several advantages over conventional suturing and stapling methods including higher speed, reduced tissue trauma, scar reduction, inflammatory response reduction, and faster healing. Moreover, major concerns about LTW carried out with laser irradiation alone include low effectiveness and peripheral tis-

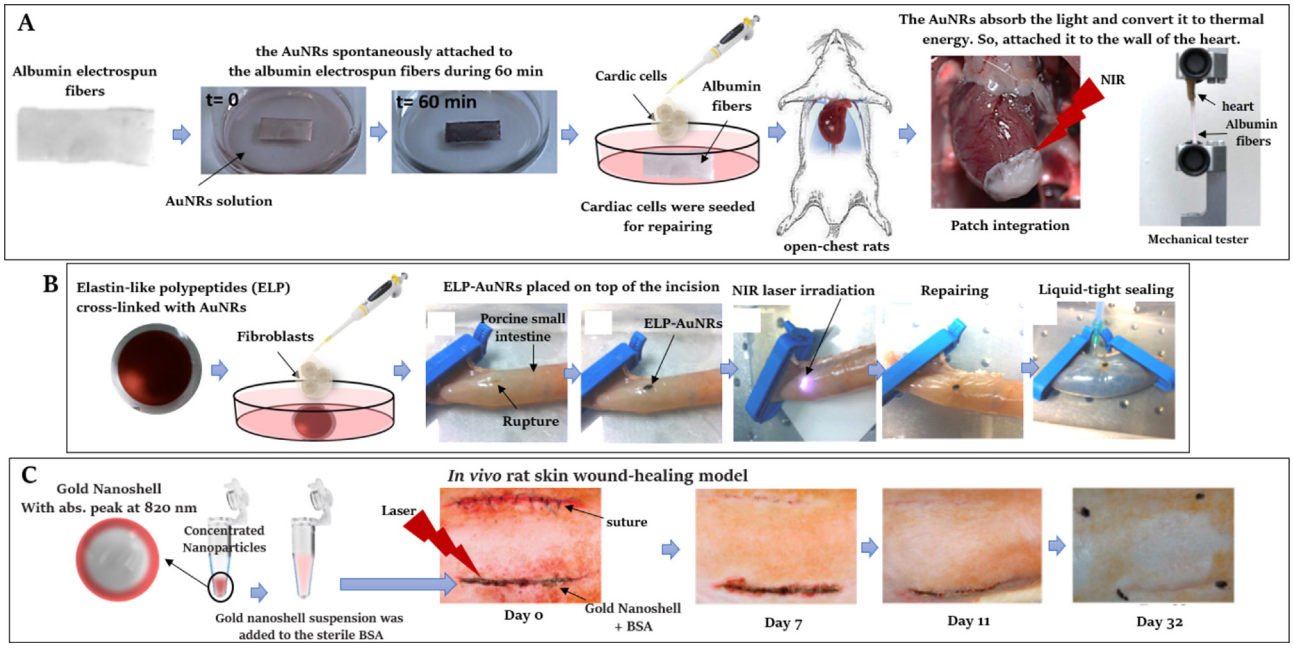

Fig. 9. (A) Gold nanorods adsorption to albumin electrospun fiber scaffolds to form cardiac patch, the cardiac cells were seeded into scaffold. Finally the patch is placed on the heart and irradiated with an 808 nm laser (tissue adhesion was assessed by a mechanical tester). (B) Gold nanorods were added into the polypeptide scaffold and then composite was applied to the rupture site of intestine. Laser irradiation provided optimal tissue welding and resulted in tissue leaking recovery. (C) Photographs of closed incisions made in rat skin from day 0 and day 32 by gold nanoshells with maximal extinction at 820 nm.

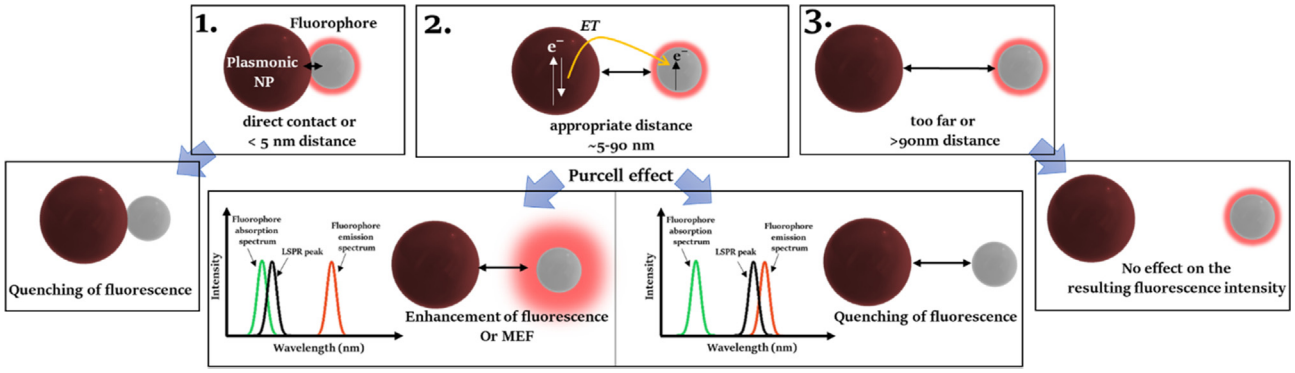

Fig. 10. The effect of distance between a fluorophore and a plasmonic NP on its fluorescence intensity.

sue thermal damage. This challenge can be addressed by using plasmonic NPs that absorb light in the laser's specific wavelength and induce a more local heating response. Their resonant extinction spectra can be tuned between 600 and 1000 nm and since most types of tissues have poor absorption between 700 and 900 nm, this ensures that the laser radiation is absorbed by plasmonic NPs, not tissue components [76,83–85]. As shown in Fig. 9A, for repairing the infarcted heart, a patch is engineered with albumin fibers and gold nanorods with plasmon resonant peak around 800 nm [84]. After near IR irradiation, the gold nanorods absorb the light and convert it to thermal energy, which locally renewed the structure of albumin fibrous, and strongly joined the patch to the wall of the heart. In another work, elastin-like polypeptides were used along with gold nanorods to weld ruptured intestinal tissue using NIR illumination (Fig. 9B) [85]. In addition, gold nanoshells have been shown to be non-cytotoxic and biocompatible as well as capable of inducing *in vivo* rat skin wound-healing model (Fig. 9C) [83].

Plasmon Resonance Energy Transfer (PRET)

Following light absorption by plasmonic NPs, Plasmon Resonance Energy Transfer (PRET) or plasmon-induced resonance energy transfer (PIRET) occurs by LSPR nonradiative decay when the resonant energy is transferred from the metal to the adjacent fluorophore [41].

Metal-enhanced fluorescence (MEF). Plasmonic NPs can effect on optical properties of nearby fluorophore [86–88]. Direct contact or less than 5 nm distance of fluorophore from NP surface leads to quenching of fluorescence (Fig. 10(1)). If a fluorophore is placed too far from NP surface there is no effect on the resulting fluorescence intensity of fluorophore (Fig. 10(3)). PRET between fluorophore and NPs as well as Purcell effect decides the enhancement or quenching effect on fluorescence intensity of fluorophore which placed at an appropriate distance from a NP surface (Fig. 10(2)). This effect is dependent on the spectral overlap between the LSPR spectrum (extinction peak) of plasmonic NP

and absorption spectrum or emission spectrum of fluorophore. Spectral overlapping between fluorophore's absorption and LSPR of NP will lead to enhanced emission of fluorophore by improving the quantum yield. This phenomenon is called metal-enhanced fluorescence (MEF) or surface-enhanced fluorescence (SEF). If LSPR spectrum overlaps the fluorescence spectrum of the fluorophore, the fluorophore will be quenched. The extent of this enhancement or quenching is related to many factors, such as size and shape of the NPs, the orientation of the fluorophore dipole moments, the organic solvents and quantum yield of the fluorophore.

Summary and outlook

In summary, we have portrayed a comprehensive understanding of plasmonic materials for applications in medicine and tissue engineering. Main aspects of the current review are (1) Considerable attention to physicochemical aspects of plasmonic nanoparticles and their connection to sensing, imaging, labeling, therapy, drug delivery and tissue engineering. (2) This review thoroughly surveys all of the opportunities and challenges associated with clinical translations and plasmonic nanomaterials. (3) The reader can choose the best nanoparticle needed to carry out his project in the field of diagnostic, therapeutic, or biomedical engineering. (4) Results of clinical trials obtained with plasmonic nanomaterials highlights the potential advantages and future directions in clinical translations. (5) All of the overriding principles that govern the successful design of plasmonic nanomaterial-based biomedical engineering are schematically summarized.

Compliance with Ethics Requirements

This article does not contain any studies with human or animal subjects.

CRediT authorship contribution statement

Yasaman-Sadat Borghei: Methodology, Conceptualization, Formal analysis, Investigation, Data curation, Writing – original draft, Visualization. **Saman Hosseinkhani:** Formal analysis, Validation, Writing – review & editing, Data curation, Supervision. **Mohammad Reza Ganjali:** Data curation, Supervision.

Declaration of Competing Interest

The authors declare that they have no known competing financial interests or personal relationships that could have appeared to influence the work reported in this paper.

References

[1] Khlebtsov NG, Dykman LA. In: Handbook of photonics for biomedical science; CRC Press. 2010. p. 73–122.
[2] Lim WQ, Gao Z. Nano Today 2016;11:168–88.
[3] Park JE, Kim M, Hwang JH. J M Nam 2017:1600032.
[4] Lee S, Sun Y, Cao Y, Kang SH. TrAC, Trends Anal Chem 2019;117:58–68.
[5] Kaushal S, Nanda SS, Samal S, Yi DK. ChemBioChem 2020;21:576–600.
[6] Nguyen HH, Park J, Kang S, Kim M. Sensors 2015;15:10481–510.
[7] Jatschka J, Dathe A, Csáki A, Fritzsche W, Stranik O. Sens Bio-Sens Res 2016;7:62–70.
[8] Petryayeva E, Krull UJ. Anal Chim Acta 2011;706:8–24.
[9] Huang X, El-Sayed MA. J Adv Res 2010;1:13–28.
[10] Singh P. Rev Plasmonics 2017;2016:211–38.
[11] Boken J, Khurana P, Thatai S, Kumar D, Prasad S. Appl Spectrosc Rev 2017;52:774–820.
[12] Liu J, He H, Xiao D, Yin S, Ji W, Jiang S, et al. Materials 2018;11:1833.
[13] Borghei YS, Hosseini M, Dadmehr M, Hosseinkhani S, Ganjali MR, Sheikhnejad R. Anal Chim Acta 2016;904:92–7.
[14] Borghei YS, Hosseini M, Ganjali MR, Ju H. Microchim Acta 2018;185:1–9.
[15] Borghei YS, Hosseinkhani S. Talanta 2020;208:120463.
[16] Zhang N, Han C, Fu X, Xu YJ. Chem 2018;4:1832–61.
[17] Erwin WR, Zarick HF, Talbert EM, Bardhan R. Energy Environ Sci 2016;9:1577–601.
[18] Huang HJ, Wu JCS, Chiang HP, Chou Chau YF, Lin YS, Wang YH, et al. Catalysts 2020;10:46.
[19] Ma XC, Dai Y, Yu L, Huang BB. Light Sci Appl 2016;5.
[20] Krajczewski J, Kołątaj K, Kudelski A. RSC Adv 2017;7:17559–76.
[21] Roy S, Jaiswal A. In: Next Generation Point-of-care Biomedical Sensors Technologies for Cancer Diagnosis. Singapore: Springer; 2017. p. 173–204.
[22] Hamm L, Gee A, De Silva Indrasekara AS. Appl Sci 2019;9:1448.
[23] Park H, Lee S, Chen L, Lee EK, Shin SY, Lee YH, et al. PCCP 2009;11:7444–9.
[24] Li P, Long F, Chen W, Chen J, Chu PK, Wang H. Curr Opin Biomed Eng 2020;13:51–9.
[25] Moore TJ, Moody AS, Payne TD, Sarabia GM, Daniel AR, Sharma B. Biosensors 2018;8:46.
[26] Liu Y, Ashton JR, Moding EJ, Yuan H, Register JK, Fales AM, et al. Theranostics 2015;5:946.
[27] Soler M, Huertas CS, Lechuga LM. Expert Rev Mol Diagn 2019;19:71–81.
[28] Bibikova O, Haas J, López-Lorente ÁI, Popov A, Kinnunen M, Ryabchikov Y, et al. Anal Chim Acta 2017;990:141–9.
[29] Liu P, Zhou Y, Guo M, Yang S, Félix O, Martel D, et al. Nanoscale 2018;10:848–55.
[30] Kim M, Lin M, Son J, Xu H, Nam JM. Adv Opt Mater 2017;5:1700004.
[31] Liu M, Chao J, Deng S, Wang K, Li K, Fan C. Colloids Surf B 2014;124:111–7.
[32] Khamehchian S, Nikkhah M, Madani R, Hosseinkhani S. J Biomed Mater Res Part A 2016;104:2693–700.
[33] Kim J, Chhour P, Hsu J, Litt HI, Ferrari VA, Popovtzer R, et al. Bioconjug Chem 2017;28:1581–97.
[34] Meir R, Motiei M, Popovtzer R. Nanomedicine 2014;9:2059–69.
[35] Varna M, Xuan HV, Fort E. Wiley Interdiscip Rev Nanomed Nanobiotechnol 2018;10:e1470.
[36] Mahan MM, Doiron AL. J Nanomater 2018;2018.
[37] Cole LE, Ross RD, Tilley JM, Vargo-Gogola T, Roeder RK. Nanomedicine 2015;10:321–41.
[38] Karunamuni R, Naha PC, Lau KC, Al-Zaki A, Popov AV, Delikatny EJ, et al. Eur Radiol 2016;26:3301–9.
[39] Curry T, Kopelman R, Shilo M, Popovtzer R. Contrast Media Mol Imaging 2014;9:53–61.
[40] Naha PC, Lau KC, Hsu JC, Hajfathalian M, Mian S, Chhour P, et al. Nanoscale 2016;8:13740–54.
[41] Lee SW, Hong JW, Lee H, Wi DH, Kim SM, Han SW, et al. Nanoscale 2018;10:10835–43.
[42] Kim M, Lee JH, Nam JM. Adv Sci 2019;6:1900471.
[43] Gao L, Liu M, Ma G, Wang Y, Zhao L, Yuan Q, et al. ACS Nano 2015;9:10979–90.
[44] Ge C, Fang G, Shen X, Chong Y, Wamer WG, Gao X, et al. ACS Nano 2016;10:10436–45.
[45] Zhang Y, Jin Y, Cui H, Yan X, Fan K. RSC Adv 2020;10:10–20.
[46] Liang M, Yan X. Acc Chem Res 2019;52:2190–200.
[47] He W, Liu Y, Yuan J, Yin JJ, Wu X, Hu X, et al. Biomaterials 2011;32:1139–47.
[48] Han J, Zhang L, Hu L, Xing K, Lu X, Huang Y, et al. J Dairy Sci 2018;101:5770–9.
[49] Cai S, Jia X, Han Q, Yan X, Yang R, Wang C. Nano Res 2017;10:2056–69.
[50] Cormode DP, Gao L, Koo H. Trends Biotechnol 2018;36:15–29.
[51] Li Y, Yun KH, Lee H, Goh SH, Suh YG, Choi Y. Biomaterials 2019;197:12–9.
[52] Flores-López LZ, Espinoza-Gómez H, Somanathan R. J Appl Toxicol 2019;39:16–26.
[53] Fathi-Achachelouei M, Knopf-Marques H, Ribeiro da Silva CE, Barthès J, Bat E, Tezcaner A, et al. Front Bioeng Biotechnol 2019;7:113.
[54] Mihai MM, Dima MB, Dima B, Holban AM. Materials 2019;12:2176.
[55] Kaundal V, Sharma V. Int Surg J 2019;6:2973–5.
[56] Choudhury H, Pandey M, Lim YQ, Low CY, Lee CT, Marilyn TCL, et al. Mater Sci Eng, C 2020;112:110925.
[57] Yadid M, Feiner R, Dvir T. Nano Lett 2019;19:2198–206.
[58] Tian J, Wong KK, Ho CM, Lok CN, Yu WY, Che CM, et al. Drug Discovery 2007;2:129–36.
[59] Nguyen VN, Qi S, Kim S, Kwon N, Kim G, Yim Y, et al. J Am Chem Soc 2019;141:16243–8.
[60] Chadwick SJ, Salah D, Livesey PM, Brust M, Volk M. J Phys Chem C 2016;120:10647–57.
[61] Stuchinskaya T, Moreno M, Cook MJ, Edwards DR, Russell DA. Photochem Photobiol Sci 2011;10:822–31.
[62] Zilio P, Dipalo M, Tantussi F, Messina GC, De Angelis F. Light Sci Appl 2017;6.
[63] Hajipour MJ, Mehrani M, Abbasi SH, Amin A, Kassaian SE, Garbern JC, et al. Chem Rev 2019;119:11352–90.
[64] Ashtari K, Nazari H, Ko H, Tebon P, Akhshik M, Akbari M, et al. Adv Drug Deliv Rev 2019;144:162–79.
[65] Shevach M, Fleischer S, Shapira A, Dvir T. Nano Lett 2014;14:5792–6.
[66] Kumar R, Aadil KR, Ranjan S, Kumar VB. J Drug Delivery Sci Technol 2020;57:101617.
[67] Nissan I, Schori H, Lipovsky A, Alon N, Gedanken A, Shefi O. J Nanopart Res 2016;18:1–10.
[68] Abdal Dayem A, Lee SB, Cho SG. Nanomaterials 2018;8:761.
[69] Niu C, Yuan K, Ma R, Gao L, Jiang W, Hu X, et al. Mol Med Rep 2017;16:4879–86.
[70] Yi C, Liu D, Fong CC, Zhang J, Yang M. ACS Nano 2010;4:6439–48.
[71] Zhang R, Lee P, Lui VC, Chen Y, Liu X, Lok CN, et al. Nanomed Nanotechnol Biol Med 2015;11:1949–59.

[72] Heo DN, Ko WK, Lee HR, Lee SJ, Lee D, Um SH, et al. J Colloid Interface Sci 2016;469:129–37.
[73] Dionne JA, Baldi A, Baum B, Ho CS, Janković V, Naik GV, et al. MRS Bull 2015;40:1138–45.
[74] Liu Y, Bhattarai P, Dai Z, Chen X. Chem Soc Rev 2019;48:2053–108.
[75] Akrami M, Balalaie S, Hosseinkhani S, Alipour M, Salehi F, Bahador A, et al. Sci Rep 2016;6:1–12.
[76] Ratto F, Matteini P, Rossi F, Menabuoni L, Tiwari N, Kulkarni SK, et al. Nanomed Nanotechnol Biol Med 2009;5:143–51.
[77] Brown E, Brunker J, Bohndiek SE. Dis Models Mech 2019;12:dmm039636.
[78] Song J, Kim J, Hwang S, Jeon M, Jeong S, Kim C, et al. Chem Commun 2016;52:8287–90.
[79] Roberts S, Andreou C, Choi C, Donabedian P, Jayaraman M, Pratt EC, et al. Chem Sci 2018;9:5646–57.
[80] Alipour M, Hosseinkhani S, Sheikhnejad R, Cheraghi R. Sci Rep 2017;7:1–13.
[81] Cheheltani R, Ezzibdeh RM, Chhour P, Pulaparthi K, Kim J, Jurcova M, et al. Biomaterials 2016;102:87–97.
[82] Lu W, Huang Q, Ku G, Wen X, Zhou M, Guzatov D, et al. Biomaterials 2010;31:2617–26.
[83] Gobin AM, O'Neal DP, Watkins DM, Halas NJ, Drezek RA, West JL. Off J Am Soc Laser Med Surg 2005;37:123–9.
[84] Malki M, Fleischer S, Shapira A, Dvir T. Nano Lett 2018;18:4069–73.
[85] Huang HC, Walker CR, Nanda A, Rege K. ACS Nano 2013;7:2988–98.
[86] Su YZ, Hung MW, Wu WH, Huang KC, Chiang HK. In: 2010 IEEE Instrumentation & Measurement Technology Conference Proceedings; 2010. p. 574–8.
[87] Park JE, Kim J, Nam JM. Chem Sci 2017;8:4696–704.
[88] Nowroozi-Nejad Z, Bahramian B, Hosseinkhani S. Enzyme Microb Technol 2019;121:59–67.

Yasaman Sadat Borghei obtained Ph.D. in nanobiotechnology in Department of Life Science Engineering, Faculty of New Sciences & Technologies, University of Tehran in 2018. Then she worked as a post-doc fellow in Prof. Hosseinkhani's lab at Tarbiat Modares University.

Mohammad Reza Ganjali is Professor of Analytical Chemistry, Head of the Centre of Excellence in Electrochemistry, and Chair professor of the College of Science at the University of Tehran, Tehran, Iran. He obtained a PhD in analytical chemistry at the University of Tehran in 1997. He has published more than 1,174 papers with 41,190 citations and an h-index of 90. He has more than 30 years of research experience in sensor and biosensor, electro-analytical chemistry, spectroscopy and nanomaterials.

Saman Hosseinkhani is Professor of Biochemistry at the Faculty of Biological Sciences, Tarbiat Modares University, Tehran, Iran. He has published more than 290 papers. He is editorial board member of some international journals. He has more than 20 years of research experience in protein engineering, bioluminescence and bio-nano interfaces.